Applied Physics Letters

Interferences in locally resonant sonic metamaterials formed from Helmholtz resonators

Cite as: Appl. Phys. Lett. **114**, 171901 (2019); https://doi.org/10.1063/1.5092375
Submitted: 11 February 2019 . Accepted: 16 April 2019 . Published Online: 01 May 2019

María Pilar Peiró-Torres, Sergio Castiñeira-Ibáñez, Javier Redondo, and Juan Vicente Sánchez-Pérez

Applied Physics Letters ARTICLE scitation.org/journal/apl

Interferences in locally resonant sonic metamaterials formed from Helmholtz resonators

Cite as: Appl. Phys. Lett. **114**, 171901 (2019); doi: 10.1063/1.5092375
Submitted: 11 February 2019 · Accepted: 16 April 2019 ·
Published Online: 1 May 2019

María Pilar Peiró-Torres,[1,2] Sergio Castiñeira-Ibáñez,[2,3] Javier Redondo,[4] and Juan Vicente Sánchez-Pérez[2,a)]

AFFILIATIONS

[1]BECSA, Ciudad del Transporte II, C/Grecia, 31, 12006 Castellón, Spain
[2]Centro de Tecnologías Físicas, Acústica, Materiales y Astrofísica, Universitat Politècnica de València, División acústica, Camino de Vera s/n, 46022 Valencia, Spain
[3]Departamento de Ingeniería Electrónica, Universitat de València, Avda. Universidad s/n Bujassot, 46100 Valencia, Spain
[4]Instituto de Investigación para la Gestión Integrada de zonas Costeras, Universitat Politècnica de València, Paranimf 1, Grao de Gandia, 46730 Gandia, Valencia, Spain

[a)]jusanc@fis.upv.es

ABSTRACT

The emergence of materials artificially designed to control the transmission of waves, generally called metamaterials, has been a hot topic in the field of acoustics for several years. The design of these metamaterials is usually carried out by overlapping different wave control mechanisms. An example of this trend is the so-called Locally Resonant Sonic Materials, being one of them the Phononic Crystals with a local resonant structure. These metamaterials are formed by sets of isolated resonators in such a way that the control of the waves is carried out by resonances and by the existence of Bragg bandgaps, which appear due to the ordered distribution of the resonators. Their use is based on the creation of resonance peaks to form additional nontransmission bands mainly in the low frequency regime, usually below the first Bragg frequency. The coupling of both gaps has been made in some cases, but it is not always so. In this work, using a periodic structure formed by Helmholtz resonators, we report the existence of interferences between the resonances and the Bragg bandgaps when they are working in nearby frequency ranges, so that they prevent the coupling of both gaps. We explain their physical principles and present possible solutions to mitigate them. To this end, we have developed numerical models based on the finite element method, and the results have been verified by means of accurate experimental results obtained under controlled conditions.

Acoustic metamaterials are defined as artificial structures with physical effective properties, related to the control of elastic waves, not found in nature. In the past decade, a great effort has been made in order to analyze their rich physics and the large number of potential applications.[1–16] An important kind of acoustic metamaterial is that formed by Phononic Crystals (PCs) with a locally resonant structure, formed by periodic arrays of Helmholtz Resonators (HRs).[17–22] These metamaterials are included inside the well-known Locally Resonant Sonic Materials (LRSMs).[11,23–25] In these crystalline metamaterials, the existence of Bragg gaps (BGs) in the low frequency regime is restricted due to the requirement of dimensional similarity between wavelengths and the lattice constant of PC. Nevertheless, this limitation is overcome with the creation of subwavelength Locally Resonant bandgaps (LRGs), through the inclusion of HR in the array. Although BG and LRG are usually far from each other in the domain of frequencies, in some cases, the coupling of both gaps is interesting to obtain a broadband transmission loss. This possibility has already been analyzed for other LRSM configurations[26] different from those analyzed here. However, in the case of using HR, there are some different interactions between BG and LRG that, having been reported by some authors[18,27] as a part of papers focused on other purposes, have not yet been analyzed in depth.

In this work, we study the underlying Physics in BG/LRG interactions using a simplified two-dimensional (2D) numerical model based on the Finite Element Method (FEM) and supporting the obtained results with accurate experiments carried out under controlled conditions. This study is focused on the case of 2DPC formed by rigid scatterers in air, usually called Sonic Crystals.[28,29]

To analyze these interactions, we have developed the geometry shown at the top of Fig. 1(a). The considered 2D domain of length $L = 1$ m is formed by 3 scatterers with external (internal) radius, r_{ext} (r_{int}), and separated by the lattice constant of the array formed, a. The

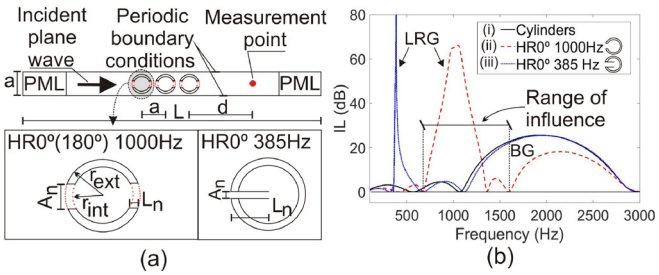

FIG. 1. (a) Numerical 2D model to analyze the BG/LRG interactions. The typology of the scatterers is shown at the bottom; (b) IL spectra for the three considered arrays.

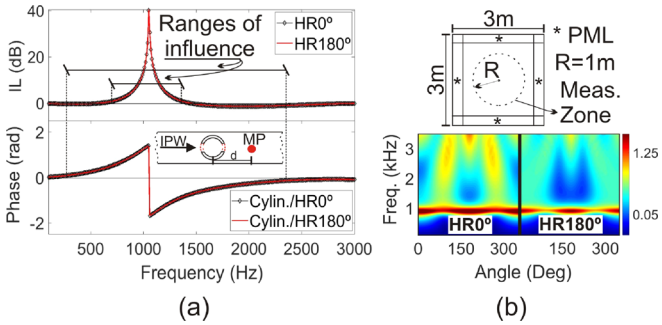

FIG. 2. Analysis of the influence of the three possible mechanisms responsible for interference in the case of single scatterers; (a) absorption spectra (upper part) and phase shift spectra (lower part) for HR0° and HR180°. In the inset, you can see a schematic of the numerical model used; (b) an outline of the anechoic model used to simulate the directivity of both HR (upper part); the directivity results can be seen at the bottom.

scatterers can work as closed cylinders or cylindrical HR with a cross-sectional area of the neck, A_n, and length of the neck, L_n. HR can be placed in the numerical domain with the necks oriented in any direction, but for the sake of brevity, we will analyze here only two cases: 0° and 180° with respect to the direction of propagation of an incident plane wave traveling from left to right, calling hereinafter HR0° and HR180°, respectively. In all cases, the scatterers are confined between two linear boundaries separated by the lattice constant of the array, a. The measurement point is located at d = 0.2 m from the center of the last scatterer, far enough to avoid near-field effects behind the sample. The vertical boundaries are surrounded by Perfectly Matched Layers (PMLs)[30] to simulate the Sommerfeld radiation conditions. In the horizontal boundaries of the model, we have imposed periodic boundary conditions. Considering these conditions, the incident wave is not reflected by the horizontal boundaries, but the scattered waves reproduce the effect of a semi-infinite 2D Sonic Crystal formed by 3 rows of scatterers arranged in a square array. Finally, since we have considered all types of scatterers to be acoustically rigid, the Neumann boundary condition (zero sound velocity) is applied to their surfaces.

To visualize first the LRG/BG acoustic interactions, we have considered an array with a BG centered at 2000 Hz with three different kinds of scatterers: (i) cylinders; (ii) HR0° with a LRG centered at 1000 Hz; and (iii) HR0° with a LRG at 385 Hz. The values of the general parameters of the array are a = 0.08 m, r_{ext} = 0.0315 m, and r_{int} = 0.0257 m, being the particular values for each HR0° L_n = 0.0058 m (0.04 m) and A_n = 0.02 m (0.004 m) for the second and the third cases, respectively. The details are presented at the bottom of Fig. 1(a). In all cases, the attenuation spectrum, usually called Insertion Loss (IL), has been calculated. The obtained results are presented in Fig. 1(b). It can be observed that when the LRG is far from the BG in the frequency domain [array (i) vs array (iii)], the size of the BG is almost equal, being the BG/LRG interaction almost negligible. However, when BG and LRG are close [array (i) vs array (ii)], a reduction in the BG appears, which would be greater if LRG and BG are closer. In the latter case, the range of influence of the interference extends to a larger frequency range than that occupied by the LRG itself.

The interference produced in the transmitted field considering only a single scatterer has been analyzed first. Three would be the potential mechanisms involved: (i) the absorption, (ii) a change in directivity, or (iii) a phase shift. The first and third mechanisms have been analyzed using a numerical model that simulates an impedance tube with anechoic ends, as can be seen in the inset of Fig. 2(a), while the scheme shown at the top of Fig. 2(b), which consists of a typical anechoic configuration used to measure the directivity of the scattered field, has been numerically developed to analyze the change in the directivity. In the latter model, a plane wave traveling from left to right impinges on each of the considered scatterers located in the center of the domain, allowing us to estimate the scattered field in the circular measurement zone.

Concerning the absorption, at the top of Fig. 2(a), it can be seen that the IL spectra for a single HR0° (HR180°) are exactly the same, showing the resonance peak centered at 1000 Hz. But its range of affectation in the frequency domain does not correspond to the interference phenomenon to be analyzed, which affects a larger frequency range outside the absorption itself, as can be seen in Fig. 1(b) for the HR0°1000Hz case. This result allows us to rule out absorption as the main mechanism responsible for interference. In the case of the change in the directivity, the results are shown at the bottom of Fig. 2(b), where the sound pressure scattered by both HR0° and HR180° is presented. It can be seen that both sound fields are completely different being their IL spectra exactly the same, as stated above. That means that the directivity does not affect the attenuation produced by HR, and this result allows us to discard the directivity mechanism as well. Finally, the results of the Cylinder/HR0° and Cylinder/HR180° phase shifts are shown at the bottom of Fig. 2(b). One can observe that both spectra are equal, being this mechanism compatible with the range of influence shown in Fig. 1(b). Then, we can conclude that the phase shift could be the main responsible for this interference.

Next, we will focus our analysis on the physics involved in the phase shift mechanism for a single scatterer, considering first the phenomenon of resonance in isolation, without scattering. For this, we use the numerical model presented at the top of Fig. 3(a), which considers a single HR not located in the transmitted wave path. The numerical domain consists of a rectangle with rigid boundaries, and an HR with dimensions a = 0.04 m, b = 0.03 m, c = 0.01 m, and d = 0.01 m, which supposes a resonance peak at 1000 Hz, is considered. An incident plane wave traveling from left to right is reflected at the rigid right boundary, and the sound pressure level is measured in a point located at e = 0.85 m from this boundary. The results can be seen at the bottom of Fig. 3(a). In the absence of the HR, the eigenmodes would appear for frequencies given by

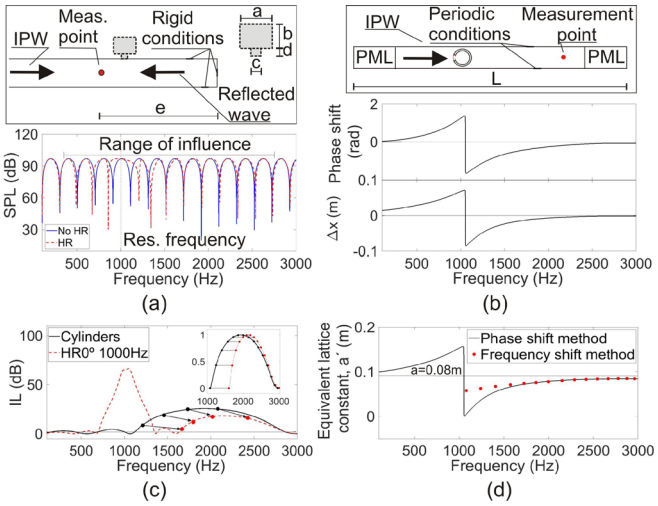

FIG. 3. Analysis of the influence of the phase shift on the BG/LRG interference; (a) Phase shift for the pure resonance case for a single HR. An outline of the model is presented at the top. The variation of Sound Pressure Level (SPL) is presented at the bottom; (b) phase shift for the case of resonance plus scattering for a single scatterer. The numerical model is presented at the upper part. At the center, the phase shift Cylinder/HR0° is shown. The lower part represents the distance displacement, Δx, associated with the phase shift; (c) BG/LRG interference, showing with arrows the displacement of frequencies in the BG. The normalization to 1 of the BG for both arrays formed either by cylinders or by HR0° can be seen in the inset; (d) ELC as a function of frequency, calculated from the phase shift (continuous black line) and frequency shift (red dotted line).

$$f = nc/(2L), \tag{1}$$

where n is an integer, c is the speed of sound, and L is the length of the domain. However, in the presence of HR, the eigenmodes are displaced within a frequency range around the resonance frequency of the HR. Thus, within the range of influence of the HR, the modes are shifted forward or backward for frequencies below or above the resonance frequency, respectively.

The next step is the analysis of the resonance along with the scattering by adapting the model of Fig. 1(a) to the case of a single scatterer [top of Fig. 3(b)] and determining the phase shift of the transmitted wave at the measurement point. The phase shift is presented at the middle of Fig. 3(b), and one can check that the range of influence is similar to both the previous case and the one shown in Fig. 1(b). Note that the interference phenomenon reported here would exist in the frequency range in which the phase shift exists. This range is indicated in the lower part of Fig. 2(b) for the case of a single resonator (called "range of influence") and in Fig. 3(d) for the case of LRSM (from below 100 Hz to above 3000 Hz). This phase shift can be interpreted as a difference of distances, in which the transmitted wave in both HR0° and cylinder cases would have the same phase state. Thus, a distance shift, Δx, can be easily calculated as a function of the frequency, f, and the phase shift previously obtained, φ, as follows:

$$\Delta x = \varphi c/2\pi f. \tag{2}$$

The absolute value of Δx has a maximum at the resonance frequency and decreases as we move away from it, maintaining in a range of influence at both higher and lower frequencies, as shown at the bottom of Fig. 3(b).

The concept of distance shift becomes important when applied to the case of PC, where the BG appears. In these devices, the location of the BG depends on the lattice constant of the array, which in turn determines the position of the scatterers. Due to the phase shift induced by the HR, the waves would arrive to the scatterers in a different state of phase, and Δx could be understood as if the lattice constants considering either HR0° or cylinders were different. In other words, the BG/LRG interference makes the distance between scatterers seen by the wave, a′, different from the real one, a. This means that the BG is not destroyed, but shifted to another range of frequencies. If we consider the HR°1000 Hz array with a = 0.08 m, where the BG/LRG interference is more noticeable, this fact is presented in Fig. 3(c) where the displacement of frequencies in the BG is marked with arrows. In the following, we will name a′ as the "Equivalent Lattice Constant" (ELC).

Two different methods to estimate the trend of variation of the ELC as a function of frequency have been considered. The first is the phase shift method, already used in the case of a single scatterer, applied to the case of the considered PC. The second is the frequency shift method, in which both BG are normalized to 1 [see the inset of Fig. 3(c)], and from the frequency shift between both BG, the corresponding ELC is estimated. The results for some frequencies above the resonance peak are presented in Fig. 3(d) on the basis of the starting value of a (a = 0.08 m). The same trend is observed with both methods, equal to the case of a single scatterer, where there is a variation in the ELC in the range of influence of the HR. In the example considered, the BG of the HR0° array moves toward high frequencies because $a' < a$ since the BG is above the LRG. Due to the fact that a′ depends on the frequency, an increase in the real lattice constant would compensate the effect of the phase shift induced by HR0° and would produce a displacement of the BG again toward low frequencies. Similarly, if the BG were located below the resonance peak, $a' > a$, and the BG would shift to low frequencies. To correct this, the value of the real lattice constant should be decreased.

To validate these numerical predictions, we have carried out accurate experiments in an anechoic chamber using a directional white sound source (S) and measuring at a distance d = 1 m behind the sample. In the inset of Fig. 4, we show an outline of the experimental setup used. A comparison between the numerical and experimental IL results for three cases can be seen in Fig. 4: At the top, a PC with closed cylinders with a = 0.08 m, where the first BG is centered at 2000 Hz

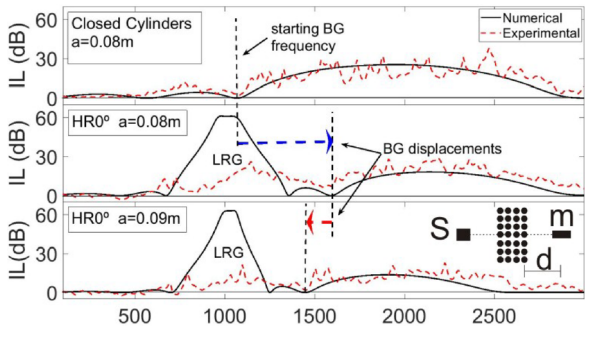

FIG. 4. Numerical (continuous black line) vs experimental (red dashed line) IL results for three PC cases: Cylinders with a = 0.08 m, HR0° with a = 0.08 m, and HR0° with a = 0.09 m. An outline of the experimental setup is shown at the bottom left.

and starting around 1050 Hz, is observed. At the middle, a PC made of HR0° 1000 Hz, where the displacement of the first BG, which now starts around 1550 Hz, is observed. At the bottom, one can see a PC with HR0° but with a higher lattice constant (a = 0.09 m), where the first BG has moved toward low frequencies, starting at 1450 Hz. In the latter case, the size of the starting BG has not been completely recovered, and only its position in the frequency range due to the increase in the lattice constant that reduces the filling fraction of the PC is recovered. The experimental results are in quite good agreement with the numerical simulations, considering the use of an ideal numerical model. Note that although the ELC is a function of frequency, a single variation of the lattice constant produces the displacement of the BG.

In summary, in this work, we have analyzed in depth the BG/LRG interference phenomenon in PC formed by HR. We have performed numerical simulations validated with accurate experiments carried out under controlled conditions. The placement of HR as scatterers, when the LRG is close to BG, induces a phase shift in the transmitted wave that can be understood as a virtual change in the lattice constant of the array, which is greater or smaller than the real one depending on the relative position of the BG with respect to the LRG in the frequency domain. This virtual lattice constant has been named the Equivalent Lattice Constant (ELC) by us.

M.P.P.T. is grateful for the support of pre-doctoral Grant by the "Ministerio de Economía y Competitividad" of Spain through reference No. DI-15-08100.

REFERENCES

[1]L. Fok, M. Ambati, and X. Zhang, "Acoustic metamaterials," MRS Bull. **33**, 931 (2008).
[2]J. Christensen, V. Romero-García, R. Picó, A. Cebrecos, F. G. De abajo, N. A. Mortensen, M. Willatzen, and V. Sánchez-Morcillo, Sci. Rep. **4**, 4674 (2014).
[3]Z. Liang, M. Willatzen, J. Li, and J. Christensen, Sci. Rep. **2**, 859 (2012).
[4]J. Mei, G. Ma, M. Yang, Z. Yang, W. Wen, and P. Sheng, Nat. Commun. **3**, 756 (2012).
[5]S. H. Lee, C. M. Park, Y. M. Seo, Z. G. Wang, and C. K. Kim, Phys. Rev. Lett. **104**, 054301 (2010).
[6]R. Fleury, D. L. Sounas, C. F. Sieck, M. R. Haberman, and A. Alu, Science **343**, 516 (2014).
[7]Y. Cheng, J. Y. Xu, and X. J. Liu, Phys. Rev. B **77**, 045134 (2008).
[8]Y. Cheng, F. Yang, J. Y. Xu, and X. J. Liu, Appl. Phys. Lett. **92**, 151913 (2008).
[9]L. Sanchis, V. M. García-Chocano, R. Llopis-Pontiveros, A. Climente, J. Martínez-Pastor, F. Cervcera, and J. Sánchez-Dehesa, Phys. Rev. Lett. **110**, 124301 (2013).
[10]M. Farhat, P. Y. Chen, H. Bağcı, S. Enoch, S. Guenneau, and A. Alu, Sci. Rep. **4**, 4644 (2014).
[11]N. Fang, D. Xi, J. Xu, M. Ambati, W. Srituravanich, C. Sun, and X. Zhang, Nat. Mater. **5**(6), 452 (2006).
[12]C. Shen, J. Xu, N. X. Fang, and Y. Jing, Phys. Rev. X **4**(4), 041033 (2014).
[13]Y. Li, B. Liang, X. Y. Zou, and J. C. Cheng, Appl. Phys. Lett. **103**(6), 063509 (2013).
[14]K. Tang, C. Qiu, J. Lu, M. Ke, and Z. Liu, J. Appl. Phys. **117**(2), 024503 (2015).
[15]X. Cai, Q. Guo, G. Hu, and J. Yang, Appl. Phys. Lett. **105**(12), 121901 (2014).
[16]V. Leroy, A. Strybulevych, M. Lanoy, F. Lemoult, A. Tourin, and J. H. Page, Phys. Rev. B **91**(2), 020301 (2015).
[17]X. Hu and C. T. Chan, Phys. Rev. E **71**(5), 055601 (2005).
[18]M. Karimi, P. Croaker, and N. Kessissoglou, J. Acoust. Soc. Am. **141**(1), 313 (2017).
[19]X. W. Yang, J. S. Lee, and Y. Y. Kim, J. Sound Vib. **383**, 89 (2016).
[20]Y. Chen and L. Wang, Appl. Phys. Lett. **105**(19), 191907 (2014).
[21]G. Theocharis, O. Richoux, V. Romero-García, A. Merkel, and V. Tournat, New J. Phys. **16**(9), 093017 (2014).
[22]A. Lardeau, J. P. Groby, and V. Romero-Garcia, Crystals **6**(5), 51 (2016).
[23]Z. Liu, X. Zhang, Y. Mao, Y. Y. Zhu, Z. Yang, C. T. Chan, and P. Sheng, Science **289**(5485), 1734 (2000).
[24]C. M. Park and S. H. Lee, Appl. Phys. Lett. **102**(24), 241906 (2013).
[25]T. T. Wang, Y. F. Wang, Y. S. Wang, and V. Laude, Appl. Phys. Lett. **113**(23), 231901 (2018).
[26]B. Yuan, V. F. Humphrey, J. Wen, and X. Wen, Ultrasonics **53**, 1332–1343 (2013).
[27]F. Montiel, H. Chung, M. Karimi, and N. Kessissoglou, Wave Motion **70**, 135 (2017).
[28]M. M. Sigalas, E. N. Economou, and M. Kafesaki, Phys. Rev. B **50**, 3393 (1994).
[29]E. N. Economou and M. M. Sigalas, Phys. Rev. B **48**(18), 13434 (1993).
[30]J. P. Berenguer, J. Comput. Phys. **114**(2), 185 (1994).